Focused-Ion-Beam-Based Selective Closing and Opening of Anodic Alumina Nanochannels for the Growth of Nanowire Arrays Comprising Multiple Elements**

By *Nai-Wei Liu, Chih-Yi Liu, Huai-Hsien Wang, Chen-Feng Hsu, Ming-Yu Lai, Tung-Han Chuang,* and *Yuh-Lin Wang**

Porous anodic aluminum oxide (AAO) films have been widely used by researchers as templates for growing arrays of nanowires because their pores comprise self-aligned nano-channels with extremely high aspect ratios.[1–7] Furthermore, the nanochannels can be laterally self-organized into domains of hexagonally closed-packed (hcp) ordered arrays under certain anodization conditions.[8,9] The use of lithographic guiding techniques such as stamp nanoimprinting,[10] focused ion beam (FIB) sputtering,[11] and laser holographic print-ing[12] has extended the number of nanochannels self-organized within a single ordered domain from merely 10^2 to a tremendous number of 10^{10}. Hereafter, single-domain ideally ordered nanochannel arrays fabricated by lithographic guiding techniques are referred to simply as ordered arrays for simplicity.[13] The availability of large ordered nanochannel arrays has inspired researchers around the world to design and fabricate nanocomposites and nanodevices based on AAO templates.[4,14] One of the key steps towards the realization of the full potential of these exciting nanomaterials and better exploitation of the features of these AAO templates is to develop techniques for growing different materials in different regions of an ordered array. In previous work, a method for fabricating custom-designed arrays of nanochannels by selectively closing specific regions of the nanochannels using FIB bombardment has been reported.[15] This method facilitates the selective growth of materials within open nanochannels, enabling the creation of a nanocomposite comprising arrays of filled and empty nanochannels. In order to take full advantage of the potential of AAO templates, the ideal situation would involve filling different regions of an array with different materials. One conceptually simple and elegant method to achieve this desired objective is to open the closed nanochannels again and grow a second material into these reopened channels. Here, we report the development of a complete resist-free lithographic process for the selective closing and reopening of AAO nanochannels using FIB direct writing. We also demonstrate the potential of this method by fabricating arrays of Ag/Cu nanowires arranged in various custom-designed geometries.

The ordered nanochannel arrays used in our experiments have been prepared by a FIB lithographic guiding process, as described previously in the literature.[16] The exposure of an ordered nanochannel to a Ga FIB with different beam energies results in the formation of different surface morphologies. For example, upon exposure to a flux of 2.0×10^{16} cm^{-2} 30 keV ions, the pores of the nanochannels have been significantly reduced in size, as clearly shown by the right panel of Figure 1a. This figure shows a field-emission scanning electron micro-scopy (SEM, JEOL 6700) image of the boundary between a pristine (left) and bombarded region (right). Pore size distributions of arrays exposed to different FIB doses have been obtained by processing SEM images of the arrays using commercial software, as shown in Figure 1b. The image analysis results indicate that the average pore diameter (D) of an ordered array gradually decreases with increasing ion dose, whereas the standard deviation of the pore diameter (ΔD) tends to increase with increasing ion dose. For example, upon exposure to a 2.0×10^{16} cm^{-2} ion dose, D has been reduced by 60%, whereas $\Delta D/D$ increases from 3 to 10%. In other words, the reduction of the pore diameter by FIB bombardment compromises the uniformity of the pores on an AAO array.

Plane-view transmission electron microscopy (TEM) studies of the ion-bombarded array, as illustrated in Figure 1c, reveal that the average pore diameter of the nanochannels has been indeed reduced to 20 nm upon exposure to a dose of 2.0×10^{16} cm^{-2} ions, providing corroboration for the SEM results. Furthermore, cross-sectional TEM images (Fig. 1d) demonstrate that the reduction in the pore diameter occurs only in the top region of the nanochannels. No noticeable radiation damage or redeposition of particles sputtered from the top regions has been observed in the remaining sections of the nanochannels. Therefore, it is reasonable to conclude that

[*] Prof. Y.-L. Wang, Dr. C.-Y. Liu, C.-F. Hsu, Dr. M.-Y. Lai
Institute of Atomic and Molecular Sciences, Academia Sinica
P.O. Box 23-166, Taipei 10617 (Taiwan)
E-mail: ylwang@pub.iams.sinica.edu.tw
Prof. Y.-L. Wang, H.-H. Wang
Department of Physics, National Taiwan University
Taipei 106 (Taiwan)
N.-W. Liu, Prof. T.-H. Chuang
Department of Materials Science and Engineering
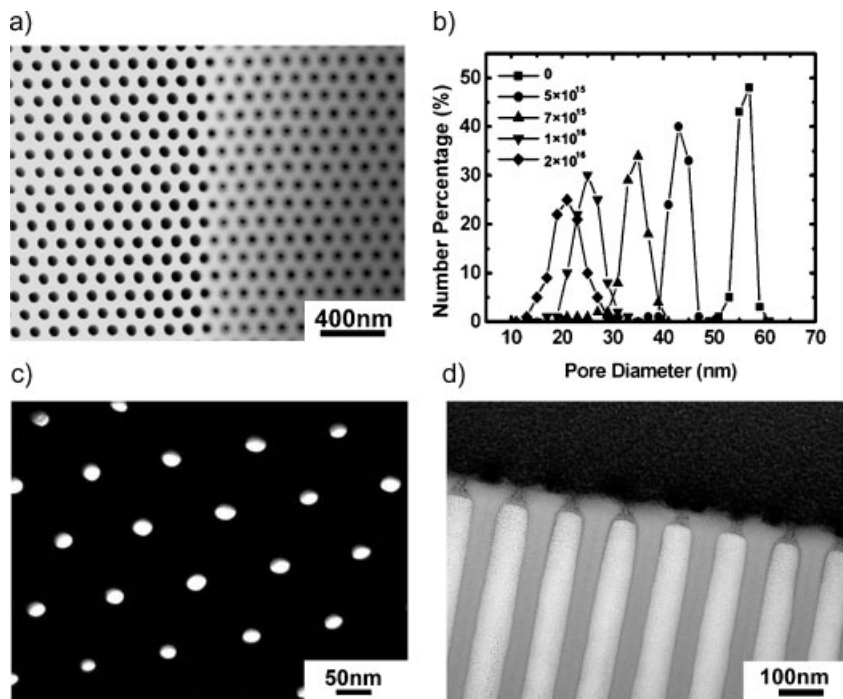National Taiwan University
Taipei 10617 (Taiwan)

a)

b)

c)

d)

Figure 1. a) Scanning electron microscopy image of the border between a pristine (left) and ion-bombarded area (right) of an ordered nanochannel array. b) Dependence of the diameter distribution on the ion dose showing the systematic reduction of the mean diameter of the nanochannels from 55 to 20 nm. Below 20 nm, some of the nanochannels are closed because of the increasing spread in distribution with increasing ion dose. c) Planar and d) cross-sectional view transmission electron microscopy images of nanochannels after exposure to an ion dose of $2.0 \times 10^{16} \, \text{cm}^{-2}$.

given energy, there exists a threshold ion dose that is required to induce the complete closure of an ordered array with a certain pore diameter (consistently 55 nm in this work); the higher the energy, the lower is the threshold. For example, the threshold doses for 40 and 20 keV ions are 2.0×10^{16} and $1.0 \times 10^{17} \, \text{cm}^{-2}$, respectively. For ions with energy below 10 keV, such a threshold does not exist because exposure to an ion dose as high as $5.0 \times 10^{18} \, \text{cm}^{-2}$ results only in partial closure of the arrays and also induces the surface morphology to become extremely rough. The changes in the surface morphology are manifested as extremely large size variations of the pores, as shown in Figure 2. The inset of Figure 2 shows that for a given ion dose of $5.0 \times 10^{18} \, \text{cm}^{-2}$, the percentage of closed nanochannels increases with increasing ion energy; furthermore, the threshold energy for complete closure of an array with 55 nm pores has been found to be 13 keV. Indeed, it has been found that the larger the size of the pores, the higher the required threshold energy. Interestingly, the inability of low-energy FIBs to completely close nanochannels holds the key to the reopening of an array that has been closed by a high-energy beam, as described in detail below.

The inset of Figure 3 shows a cross-sectional TEM image of nanochannels after exposure to $2.0 \times 10^{16} \, \text{cm}^{-2}$ of 40 keV ions. The bombarded nanochannels have been observed to be closed and capped by a 40 nm thick layer of materials that are somewhat granular in appearance. The thickness of the capping layer remains the same even after exposure to several

closure of the nanochannels is likely closely related to the redistribution of materials on the top layer of the AAO film, which is certainly a result of the collisional cascade induced by FIB bombardment.

The reduction in the pore diameter has been found to be strongly dependant on the energy of the FIB (Fig. 2). For a
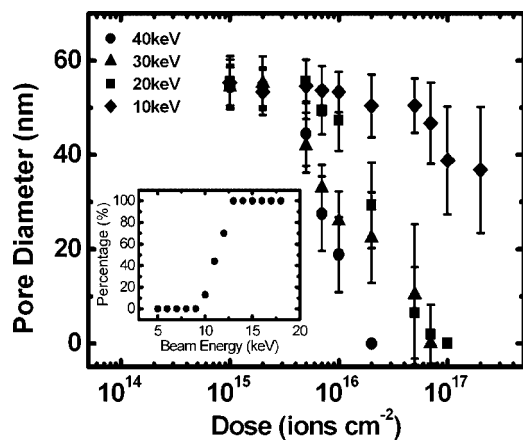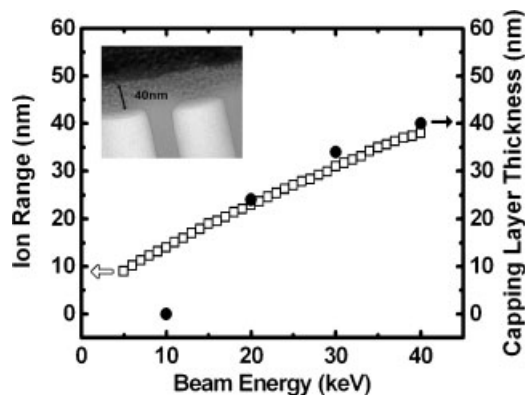

Figure 2. Dependence of the pore diameter on the ion dosage at different energies. The average diameter of the nanochannels is monotonically reduced upon exposure to various ion dosages at different energies. The inset shows the percentage of closed nanochannels plotted versus the ion energy.

Figure 3. Capping layer thickness and simulated ion range plotted versus the Ga$^+$ beam energy. The thickness of the capping layer increases with increasing beam energy; the longitudinal range of Ga$^+$ in alumina (simulated using the TRIM code) exhibits a similar dependence. The inset shows a cross-sectional TEM image of nanochannels closed using a 40 keV FIB, indicating that the thickness of the capping layer is 40 nm.
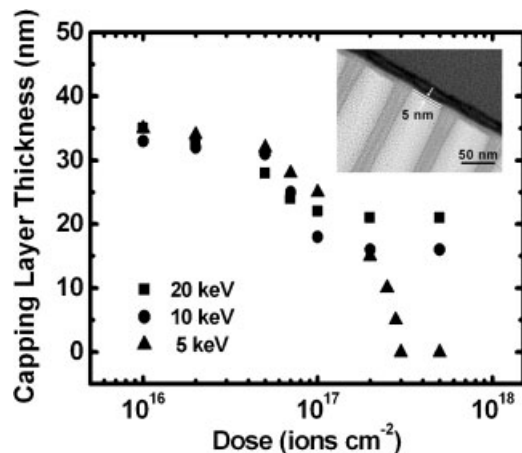
Figure 4. Reopening of closed AAO nanochannels using FIBs of different energies. The inset shows the cross-sectional TEM image of a capping layer. Capping layers as thin as 5 nm have been fabricated in the reopening process upon exposure to a dose of 2.8×10^{17} cm^{-2} of 5 keV ions.

doses of ions, indicating that the capping layer reaches a certain dynamic equilibrium thickness when the ion dose is larger than the threshold. The establishment of a dynamic equilibrium implies that the material sputtered away from the surface of the capping layer is constantly replenished by the material relocated by ion bombardment. The replenishment comes from either the redeposition of particles ejected from the sidewall of the nanochannels onto the bottom of the capping layer or the ion-induced migration of material in the capping layer.[17,18]

To shed some light into the origin of the capping layer, its thickness (d_c) has been measured as a function of the ion energy, and the results have been correlated with the simulated range (R_p) of ions in alumina,[19] as shown in Figure 3. For ion energies between 20 and 40 keV, both d_c and R_p have been found to be linearly proportional to the ion energy, and their values are essentially identical within the uncertainties of experiment and simulation. This observation strongly suggests that materials within the range of R_p are relocated by ion bombardment to maintain the equilibrium thickness of the capping layer. For ion energies below 20 keV, the average thickness of the non-uniform capping layer starts to deviate from R_p. Further reduction of the ion energy to 10 keV does not lead to any observable formation of a capping layer on the nanochannels, as indicated by the zero average thickness shown in Figure 3. The deviation of d_c from R_p at lower ion energies suggests that the materials relocated by ion bombardment are not sufficient to replenish the atoms removed from the nanochannels via sputtering. Clearly, a detailed mechanism for the ion-induced formation of the capping layer remains to be clarified by further theoretical studies, which may rely on important clues provided by the correlation between d_c and R_p, as shown in Figure 3. Since the low-energy (<10 keV) ion bombardment of an array does not lead to the formation of a capping layer, it is interesting to ask if

nanochannels that have been closed by a higher energy beam can be reopened by low-energy beam. To answer this question, an array has been first exposed to 7.0×10^{16} cm^{-2} of 30 keV ions to form a 35 nm capping layer; subsequently, the array has been exposed to ions of lower energies. Figure 4 shows the dependence of the capping layer thickness on the ion dosage for different beam energies. For 20 keV ions, the thickness decreases with increasing ion dose, finally reaching an equilibrium thickness of 21 nm, which is almost the same as achieved by bombarding a pristine array (Fig. 3). For 10 keV
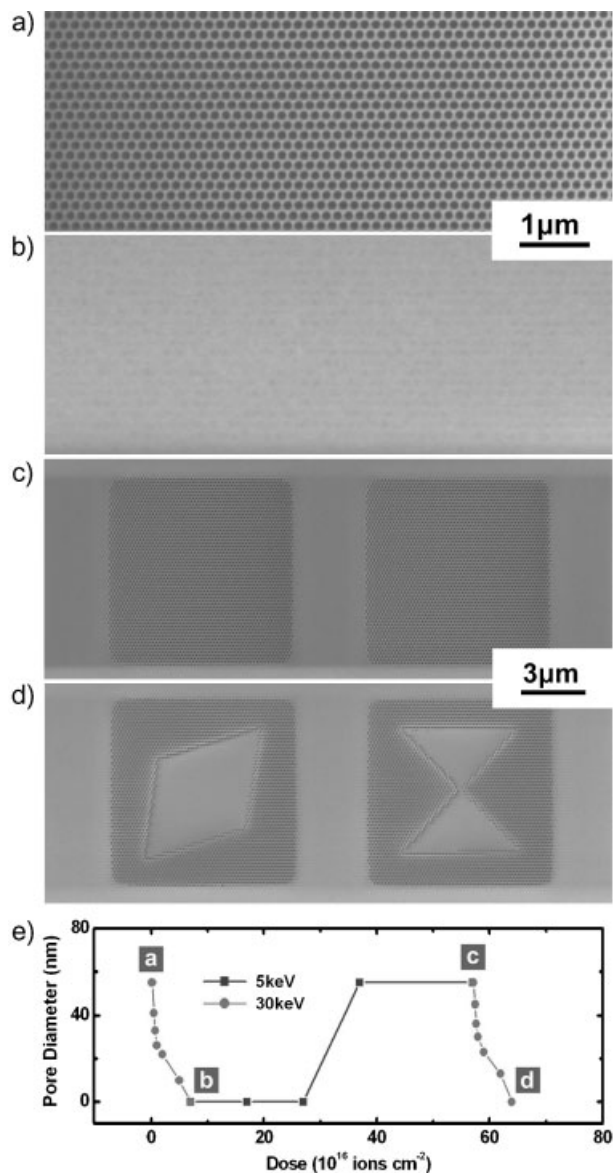

Figure 5. SEM images showing FIB-induced selective closing/opening of AAO nanochannels: a) the array before ion bombardment, b) complete closing of the array after exposure to a 30 keV FIB, c) reopening of part of the array upon 5 keV FIB bombardment, and d) closing of part of the reopened array using a 30 keV FIB. e) Plot of the average diameter of a nanochannel array as a function of the ion dose during the FIB-induced selective closing/opening process from (a) to (d).
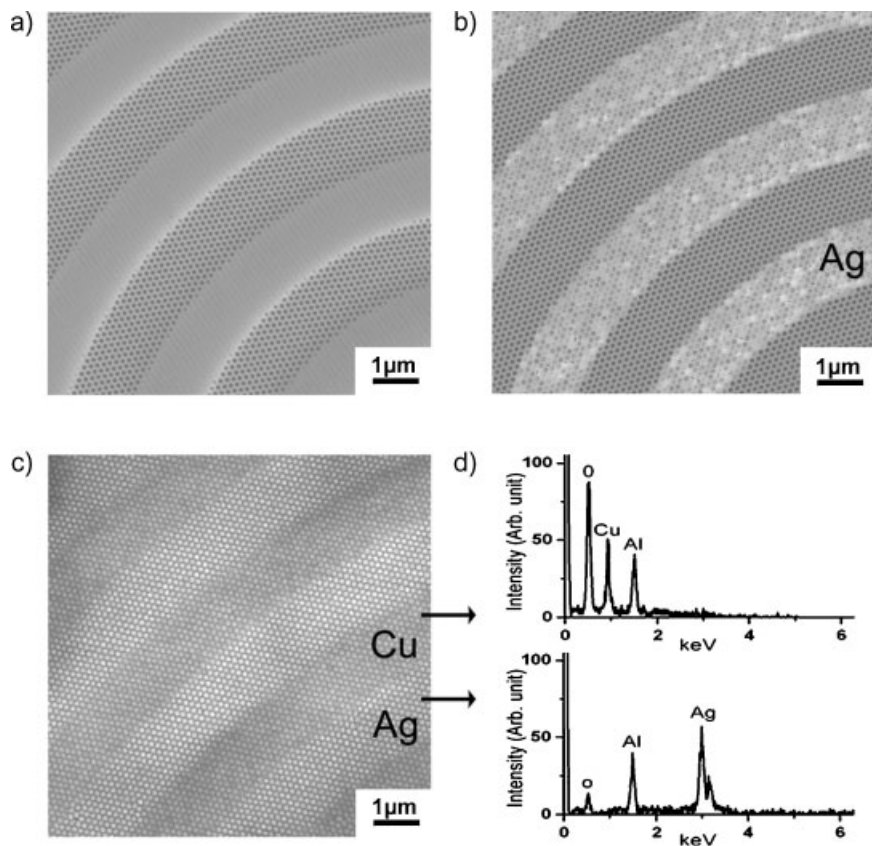
Figure 6. Selective growth of two types of nanowires within a gated nanochannel array: a) SEM image of the top region of a partially closed array. b) Top-view image of the array after growing Ag within the open nanochannels and reopening of the closed nanochannels. c) Back-view image of the array after growing Cu into the reopened nanochannels. d) Energy dispersive spectra acquired from areas containing Ag and Cu nanowires indicated in (c).

novel process to precisely fabricate an ultra-thin alumina film. The inset of Figure 4 shows a TEM image of the capping layer after exposure to $2.8 \times 10^{17}\,cm^{-2}$ of 5 keV ions. This image clearly indicates that the capping layer created by high-energy ion bombardment has been precisely thinned from 35 to 5 nm. Notably, the fabrication of such a thin continuous layer can not be achieved by the high-energy ion-beam-induced formation of a capping layer. Access to such an ultra-thin alumina film holds great promise for many potential applications.[20,21]

The successful reopening of closed nanochannels has enabled the development of an FIB-induced opening and closing process, as demonstrated in Figure 5. A long-range ordered nanochannel array (Fig. 5a) has been first closed (Fig. 5b) by subjecting it to a dose of 30 keV ions; subsequently, part of the closed array is reopened by 5 keV ion bombardment, as shown by the two square regions in Figure 5c. Finally, some of the reopened nanochannels (diamond- and sandglass-shaped regions in Fig. 5d) have been closed again by 30 keV ion bombardment. Figure 5e plots the average pore diameter of the nanochannels inside the diamond-shaped area (Fig. 5d) as a function of the cumulative ion dose to illustrate the effects of a complete cycle of FIB-induced selective nanopore closing

ions, the thickness also decreases with increasing ion dose and the equilibrium thickness is 17 nm. Indeed, this observation goes starkly against expectations, and is qualitatively very different from the results of bombarding a pristine array with ions of the same energy, which results in the partial rather than complete closure of the array. However, bombardment of a closed nanochannel array with 5 keV ions results in the complete removal of the capping layer for ion dosages higher than $3.0 \times 10^{17}\,cm^{-2}$. The observation that 10 keV ions can neither close a pristine array nor open a closed array indicates that the balance between beam-induced material relocation and sputtering is very critical for ions of this particular energy. Ions possessing this energy do not have sufficient driving force to tip the balance and change the status quo. In other words, bombardment by 10 keV ions corresponds to a bistable point for the closing or opening of nanochannels depending on the initial conditions, whereas bombardment by 5 and 20 keV ions corresponds to the exclusive opening and closing of nanochannels, respectively.

An interesting by-product of the reopening of capping layers by 5 keV ion bombardment is that this essentially provides a

and opening. It is worth noting that the FIB direct-write method does not require the use of an ion-beam resistive layer. This represents an important advantage over both photo- and electron-beam-lithography processes, which always require the application of a resistive layer to the sample surface prior to exposure. Such a layer is expected to be extremely hard to remove upon application on high-aspect-ratio nanochannels.

To demonstrate that the selective closing/opening process can be a technology platform for the growth of nanowire arrays comprising different materials, we have used a partially closed nanochannel array as a template (Fig. 6a) for growing Ag nanowires using ac electrodeposition. The growth of Ag nanowires only takes place within the open nanochannels, and no deposition of Ag has been found to occur in the closed nanochannels (Fig. 6b), indicating the effectiveness of the capping layer in blocking the growth of Ag in the closed nanochannels. After reopening of the closed nanochannels by 5 keV FIB bombardment, Cu has been electrodeposited into these nanochannels. The end product is a composite Ag—Cu nanowire array. The SEM image (Fig. 6c) and corresponding energy dispersive spectrum (Fig. 6d) of the array, measured

from the back side of the nanochannels after removal of the barrier layer, clearly show the uniformity and chemical composition of the Ag and Cu nanowires. This example demonstrates the versatility of the FIB-induced closing/opening process for the selective deposition of different materials into nanochannels arranged in a custom-designed geometry on an AAO template.

In summary, we have demonstrated a novel process to close and reopen nanochannels on an AAO film by simply bombarding its surface using FIBs with different energies. This FIB-induced closing/opening technique provides a technological platform for the selective growth of different materials in different regions of a nanochannel array upon the subsequent use of electrochemical deposition. This method thus facilitates the fabrication of nanowire arrays composed of multiple elements, which may constitute a new class of metamaterials. The small beam diameter (<10 nm) of the FIB suggests that it should be possible to selectively close an entire macroscopic array of nanochannels, leaving only a single nanochannel or a small part of the array open.[15] Such unique AAO templates may be useful as platforms for the construction of devices on the nanometer scale that can be readily connected to the macroscopic world or studied by optical probes with micrometer-scale resolution.

Experimental

High-purity (99.99%) annealed aluminum foils were electropolished in a mixed solution of 50 wt% 1:1 (v/v) $HClO_4/C_2H_5OH$ at 5 °C under constant stirring until the root mean square (rms) roughness of a typical $10 \mu m \times 10 \mu m$ area was ca. 1 nm, as measured by an atomic force microscope operated in contact mode. In order to fabricate AAO nanochannels with long-range ordering, a 50 keV Ga FIB with a diameter of ca. 10 nm and beam current of 1.1 pA was employed to create a hcp array of guiding concaves on the finely polished polycrystalline Al surface. The lattice constant was set to 100 nm in order to match the average channel spacing of a self-organized array. The array was then anodized in a 0.3 M oxalic acid solution at 3 °C at a constant voltage of 40 V. After anodization, the nanochannels were opened using a 5 wt% solution of H_3PO_4 at room temperature to obtain AAO substrates with arrays of nanochannels having the specific pore diameter and spacing required for this study.

Ion bombardments were conducted in a dual-beam FIB system (Nova 600) equipped with a SEM, which allowed for the in situ monitoring of the surface morphology of the arrays at different stages of ion exposure. The custom-designed patterns of the closed nanochannel arrays were closed at 30 keV and reopened at 5 keV FIB energies. The nanochannels in the AAO array were alternately closed or opened by changing the beam energy of the FIB.

For the growth of Ag nanowires within the AAO nanochannels, an ac (9 V) electrochemical plating procedure was employed using a mixture of silver nitrate (0.006 M) and magnesium sulfate (0.165 M) as the electrolyte. The solution had a pH value of 2, established by the addition of sulfuric acid. Cu deposition was also performed using an ac (9 V) electrochemical plating process. The electrolyte was a mixture of copper sulphate (0.2 M) and magnesium sulfate (0.08 M), and the pH value of the solution was set at 1.2.

[1] W. C. Yoo, J. K. Lee, *Adv. Mater.* **2004**, *16*, 1097.

[2] J. Choi, G. Sauer, K. Nielsch, R. B. Wehrspohn, U. Gösele, *Chem. Mater.* **2003**, *15*, 776.

[3] R. Sanz, A. Johansson, M. Skupinski, J. Jensen, G. Possnert, M. Boman, M. Vazquez, K. Hjort, *Nano Lett.* **2006**, *6*, 1065.

[4] H. Masuda, A. Abe, M. Nakao, A. Yokoo, T. Tamamura, K. Nishio, *Adv. Mater.* **2003**, *14*, 161.

[5] F. Mastumoto, M. Harada, K. Nishio, H. Masuda, *Adv. Mater.* **2005**, *17*, 1609.

[6] K. L. Hobbs, P. R. Larson, G. D. Lian, J. C. Keay, M. B. Johnson, *Nano Lett.* **2004**, *4*, 167.

[7] A. Johansson, E. Widenkvist, J. Lu, M. Boman, U. Jansson, *Nano Lett.* **2005**, *5*, 1603.

[8] H. Masuda, F. Hasegwa, S. Ono, *J. Electrochem. Soc.* **1997**, *144*, L127.

[9] A. P. Li, F. Müller, A. Birner, K. Nielsch, U. Gösele, *J. Appl. Phys.* **1998**, *84*, 6023.

[10] H. Masuda, H. Yamada, M. Satoh, H. Asoh, M. Nakao, T. Tamamura, *Appl. Phys. Lett.* **1997**, *71*, 2770.

[11] C. Y. Liu, A. Datta, Y. L. Wang, *Appl. Phys. Lett.* **2001**, *78*, 120.

[12] Z. Sun, H. K. Kim, *Appl. Phys. Lett.* **2002**, *81*, 3458.

[13] W. Lee, R. Ji, C. A. Ross, U. Gösele, K. Nielsch, *Small* **2006**, *2*, 978.

[14] H. Masuda, K. Yasui, K. Nishio, *Adv. Mater.* **2000**, *12*, 1031.

[15] N. W. Liu, A. Datta, C. Y. Liu, C. Y. Peng, H. H. Wang, Y. L. Wang, *Adv. Mater.* **2005**, *17*, 222.

[16] C. Y. Liu, A. Datta, N. W. Liu, C. Y. Peng, Y. L. Wang, *Appl. Phys. Lett.* **2004**, *84*, 2509.

[17] J. Li, D. Stein, C. McMullan, D. Branton, M. J. Aziz, J. A. Golovchenko, *Nature* **2001**, *412*, 166.

[18] T. Mitsui, D. Stein, Y. R. Kim, D. Hoogerheide, J. A. Golovchenko, *Phys. Rev. Lett.* **2006**, *96*, 036 102-1.

[19] J. F. Zeigler, J. P. Biersack, SRIM (TRIM 90), IBM Research, Yorktown, NY **1995**, This program has been used to simulate the distribution and sputtering yield of Ga^+ inside bulk alumina. The density of alumina has been set at 1.94 g cm^{-3} based on the assumption that the material is amorphous Al_2O_3 [20], as also suggested by Li et al. [22].

[20] M. Munoz, G. G. Qian, N. Karar, H. Cheng, I. G. Saveliev, N. Garcia, T. P. Moffat, P. J. Chen, L. Gan, W. F. Egelhoff, *Appl. Phys. Lett.* **2001**, *79*, 2946.

[21] H. Oshima, H. Kikuchi, H. Nakao, T. Kamimura, T. Morikawa, K. Matsumoto, J. Yuan, S. Ishio, K. Nishio, H. Masuda, K. Itoh, *IEEE Trans. Magn.* **2007**, *43*, 2148.

[22] F. Li, L. Zhang, R. M. Metzger, *Chem. Mater.* **1998**, *10*, 2470.